Available online at
http://namrc.uotechnology.edu.iq/index.php/

Nanotechnology and Advanced Materials Research Centre

Proceeding Articles Book 00 (2018) 000–000

6th International Scientific Conference on Nanotechnology, Advanced Materials and its Applications

Mixed Convective Nanofluids Laminar Flow over a Vertical Backward Facing Step with Uniform Wall Heat Flux

Ali Assim Al-Obaidi[1], Dalya Hamzah Mussa[2], Tayser Sumer Gaaz[3,*]
[1]Department of Machinery and Equipment Techniques, Technical Institute of Babylon, Al-Furat Al Awsat Technical University, Iraq
[2]Department of Electrical Power Engineering Techniques, Technical College Al-Musaib, Al-Furat Al Awsat Technical University, Iraq
[3]Department of Machinery Equipment Engineering Techniques, Technical College Al-Musaib, Al-Furat Al Awsat Technical University, Iraq
*Correspondence Author: taysersumer@gmail.com

Abstract

Numerical simulations of two-dimensional laminar mixed convection heat transfer and nanofluids flow over backward facing step in a vertical channel are numerically carried out. The continuity, momentum, and energy equations were solved by means of a finite volume method (FVM). The wall downstream of the step was maintained at a uniform wall heat flux, while the straight wall that forms the other side of the channel was maintained at a constant temperature equivalent to the inlet fluid temperature. The upstream walls of the backward-facing step were considered as adiabatic surfaces. The buoyancy assisting and buoyancy opposing flow conditions are investigated. Four different types of nanoparticles, Al_2O_3, CuO, SiO_2, and ZnO with different volumes fractions in the range of 1% to 4% and different nanoparticle diameter in the range of 25 nm to 80 nm, are dispersed in the base fluid (water) are used. The numerical results indicate that the nanofluid with SiO_2 has the highest Nusselt number compared with other nanofluids. The recirculation region and the Nusselt number increase as the step height, Reynolds number, and the volume fraction increase, and it decreases as the nanoparticle diameter increases.

Keywords: Mixed convection; backward facing step; nanofluids; channel flow

1- Introduction

The backward-facing step is a fundamental flow that provides a simple geometry to serve as a prototype which could be used to study complex phenomena such as flow separation and reattachment as recommended via previous researches [1]. The geometry of the backward-facing step classifies based on its simplicity into airfoils or three-dimensional shapes to ensure that the precise point of separation is known [2]. Simulations and measurements of flow over a backward facing step have been extensively studied in the last decades for both forced and mixed convection [4-6]. In addition, several studies tested the 3-D laminar convection flow over backward-facing step geometry [3, 4]. Numerical analysis of forced and mixed convection over horizontal and vertical backward-facing step in a duct using different nanofluids [5]. The effects of Reynolds number (in the range of $75 \leq Re \leq 225$), temperature difference (in the range of $0 \leq \Delta T \leq 30$ °C), and using nanofluid types (such as Au, Ag, Al_2O_3, Cu, CuO, diamond, SiO_2, and TiO_2) were investigated on the fluid flow and heat transfer characteristics [6]. It is found that a recirculation region developed straight behind the backward-facing step which appeared between the edge of the step and few millimeters before the corner which connects the step and the downstream wall [7]. The study of steady laminar mixed convection flow over a backward-facing step utilizing nanofluids in a two-dimensional vertical configuration under uniform heat flux boundary conditions seems not to have been investigated in the past and this has motivated the present study. Thus, the present study deals with different types of nanofluids such as (Al_2O_3, CuO, SiO_2, and ZnO) with different volume fractions and different nanoparticle diameters. The effects of

heat flux and Reynolds number on the velocity distribution, skin friction coefficient, and Nusselt number are studied and reported to illustrate the effect nanofluids on these parameters for buoyancy assisting and opposing flows.

2. Numerical Model

2.1 Physical Model

Considering the backward facing step placed in channel as shown schematically in Figure 1. The step height, and expansion ratio are fixed at 4.8 mm and 2, respectively. The upstream and downstream walls are 24 mm and 144 mm, respectively. The wall downstream of the step (X_e) is maintained at a uniform wall heat flux (q_w), while the straight wall that forms the other side of the channel is maintained at constant temperature equivalent to the inlet fluid temperature (T_o). The wall upstream of the step (X_i) and the step it-self (S) are considered as adiabatic surfaces. Nanofluids flow at the channel entrance is considered hydrodynamically steady and the fully developed flow is attained at the edge of the step, and the streamwise gradients of all quantities at the channel exit where set to be zero. The nanoparticles and the base fluid (i.e. water) are assumed to be in a thermal equilibrium and no slip condition occurs. The fluid flow is assumed to be Newtonian and incompressible. Radiation heat transfer and viscous dissipation term are neglected. The internal heat generation is not conducted in this study. The thermophysical properties of the nanofluids are assumed to be constant and it is only affected by the buoyancy force, which means that the body force acting on the fluid is the gravity; the density is varied and can be adequately modeled by the Boussinesq approximation.

2.2 Governing Equations

To complete the CFD analysis of backward facing step, it is important to set up the governing equations (continuity, momentum, and energy). Using the Boussinesq approximation and neglecting the viscous dissipation effect and compressibility effect the dimensionless governing equations for two-dimensional laminar incompressible flows can be written as follows [8]:

The continuity equation

$$\frac{\partial U}{\partial X}+\frac{\partial V}{\partial Y}=0 \qquad (1)$$

The X-momentum equation

$$U\frac{\partial U}{\partial X}+V\frac{\partial U}{\partial Y}=-\frac{\partial P}{\partial X}+\frac{\mu_{nf}}{\rho_{nf}\upsilon_{nf}}\frac{1}{Re}\left(\frac{\partial^2 U}{\partial X^2}+\frac{\partial^2 U}{\partial Y^2}\right) \qquad (2)$$

The Y-momentum equation

$$U\frac{\partial V}{\partial X}+V\frac{\partial V}{\partial Y}=-\frac{\partial P}{\partial Y}+\frac{\mu_{nf}}{\rho_{nf}\upsilon_{nf}}\frac{1}{Re}\left(\frac{\partial^2 U}{\partial X^2}+\frac{\partial^2 U}{\partial Y^2}\right)+\frac{(\rho\beta)_{nf}}{\rho_{nf}\beta_{nf}}\frac{Gr}{Re^2}\theta \qquad (3)$$

The energy equation

$$U\frac{\partial \theta}{\partial X}+V\frac{\partial \theta}{\partial Y}=\frac{\alpha_{nf}}{\alpha_f Re Pr}\left(\frac{\partial^2 \theta}{\partial X^2}+\frac{\partial^2 \theta}{\partial Y^2}\right) \qquad (4)$$

The dimensionless variables are as follows:

$$X=\frac{x}{S},\quad Y=\frac{y}{S},\theta=\frac{T-T_o}{T_w-T_o},U=\frac{u}{U_o},V=\frac{\upsilon}{U_o},$$

$$\text{and } Re=\frac{\rho u_o D_h}{\mu}$$

2.3 Boundary Conditions

The boundary conditions for the present problem that imposed at the solid walls are mainly no-slip boundary condition in addition to the specified wall temperature. The condition assumed at the inlet section are those of ambient conditions (ambient temperature and velocity) while the only condition imposed at the exit is uniform ambient pressure. The boundary conditions for the above set of governing equations are:

i. Upstream inlet conditions at

$$X=-\frac{X_i}{D_h},\frac{S}{D_h}\le Y\le\frac{H}{D_h},\text{and, } U_i=\frac{u_i}{u_o},V=0,\theta=0$$

ii. Downstream exit conditions at

$$X=\frac{X_e}{D_h},0\le Y\le\frac{H}{D_h},\text{and, }\quad\frac{\partial^2 U}{\partial X^2}=0,\quad\frac{\partial^2 V}{\partial X^2}=0,\quad\frac{\partial^2 \theta}{\partial X^2}=0$$

All the quantities at the channel exit are set to zero.

iii. Top wall conditions at

$$X=-\frac{X_i}{D_h}\le X\le\frac{X_e}{D_h},Y=\frac{H}{D_h},\text{and, } U=0,V=0,\theta=0$$

iv. Sidewalls conditions at

$$X=-\frac{X_i}{D_h}\le X\le\frac{X_e}{D_h},0\le Y\le\frac{H}{D_h},\text{and, } U=0,V=0,\theta=0$$

v. Stepped wall condition:

(a) Upstream of the step at

$$-\frac{X_i}{D_h} \le X \le 0, Y = \frac{S}{D_h}, \text{and}, U = 0, V = 0, \frac{\partial \theta}{\partial Y} = 0$$

(b) At the step

$$X = 0, 0 \le Y \le \frac{S}{D_h}, \text{and}, U = 0, V = 0, \frac{\partial \theta}{\partial Y} = 0$$

(c) Downstream of the step at

$$0 < X \le \frac{X_i}{D_h}, Y = 0, \text{and}, U = 0, V = 0, \frac{\partial \theta}{\partial Y} = -1$$

2.4 Numerical Parameters and Procedures

The numerical computation was carried out by solving the governing conservation equations along with the boundary conditions Eqs. (1) to (4). Equations for solid and fluid phase were simultaneously solved as a single domain. The discretization of governing equations in the fluid and solid regions was done using the finite-volume method (FVM). The diffusion term in the momentum and energy equations is approximated by the second-order central difference which gives a stable solution. In addition, a second-order upwind differencing scheme is adopted for the convective terms. The flow field was solved using the SIMPLE algorithm [9]. Iterative solution procedure where the computation is initialized by guessing the pressure field. Then, the momentum equation is solved to determine the velocity components. The pressure is updated using the continuity equation. Even though the continuity equation does not contain any pressure, it can be transformed easily into a pressure correction equation [10].
introduce the paper, and put a nomenclature if necessary, in a box with the same font size as the rest of the paper. The paragraphs continue from here and are only separated by headings, subheadings, images and formulae. The section headings are arranged by numbers, bold and 10 pt.

2- Results and discussion

2.5 The Effect of Nanofluids parameters

Different types of nanoparticles which are Al_2O_3, CuO, SiO_2 and ZnO and pure water as a base fluid were used. In order to see the effects of different nanofluids on the heat transfer enhancement all other parameters should be fixed, $\emptyset$ = 0.04, and d_p = 25 nm, at *Re* = 100 and q_w = 500 W/m^2 along the downstream wall. Fig. 2a shows that the Nusselt number at the heated wall increases with increasing the distance from the step to a maximum value near the step wall at some distance downstream of the reattachment point, and it then decreases slowly as the distance continues to increase in the stream wise direction. This is due to the temperature difference when the reversed flow is attached to the main separated flow which has a lower temperature. It is found that the base fluid with SiO_2 nanofluids has the highest maximum peak in Nusselt number followed by Al_2O_3, CuO, and ZnO. This is because inside the recirculation zone the nanofluid needs to have lower density & thermal conductivity. In this study, the effect of the nanoparticle volume fraction $\emptyset$ in the range of 1% to 4% on the heat transfer characteristics is studied. Fig. 2b shows the effect of different nanoparticle volume fractions on the Nusselt number for constant nanoparticle diameters d_p = 25 nm, at *Re* = 100 and q_w = 500 W/m^2. As $\emptyset$ increased, the Nusselt number of SiO_2 nanofluids becomes higher than that of pure fluids. The Hence, nanofluids with higher volume fraction bring grater heat transfer enhancement. Because increasing the volume fraction leads to increase the thermal conductivity of the fluid Fig. 2b. This happens because the temperature difference decreases as the volume fraction increases and therefore the heat transfer enhancement increases. To study the effect of the nanoparticle diameter on the heat transfer, it is evident that the Nusselt number varies significantly with the mean nanoparticle diameter between 25 - 80 nm, while Re, q_w, and $\emptyset$ are fixed at 100, 500, and 4%, respectively. The result of Nusselt number for SiO_2 nanofluids is shown in Fig. 2c. As the mean nanoparticle diameter increases, the Nusselt number decreases. Then, it is concluded that by using smaller diameter of nanoparticles will lead to get better heat transfer enhancement. The properties of nanofluid come from relatively high surface area to the volume ratio. Thus, it is concluded that by using the smaller diameter of nanoparticles will lead to getting better heat transfer enhancement. It can be observed that Nusselt number increases with decreasing the nanoparticles diameter.

2.6 The Effect of Different Reynolds Numbers

2.6.1 Velocity Distribution

The velocity distributions of SiO_2 nanofluid for different types of Reynolds numbers in the range of $100 \le Re \le 500$ with q_w = 500 W/m^2, and $\emptyset$ = 4%, and d_p = 25 nm at different *X/S* sections along the stepped wall are shown in Fig. 3. The velocity profile increases as Reynolds number increases. It is noticed that the higher Reynolds number has a higher parabolic velocity profile for SiO_2 nanofluid as shown in Fig. 3a. It is found that the velocity increases as Reynolds number increases, which enhance the recirculation size and the flow reattached farther from the step. The distance between the step and the stepped wall increases until the flow reaches the reattachment point and the size of the recirculation region decreases as shown in Figs. 3b-c. Downstream of this point, the flow starts to redevelop and then approach fully developed flow as the fluid flows towards the exit as shown in Fig. 3d.

2.6.2 Skin Friction Coefficient

The skin friction coefficient of SiO_2 nanofluid for different types of Reynolds numbers in the range of $100 \leq Re \leq 500$ with q_w = 500 W/m^2, and $\emptyset$ = 4%, and d_p = 25 nm along the downstream wall is shown in Fig. 4a. It is found that the skin friction coefficient decreases as Reynolds number increases. Moreover, it is noticed that the peaks in and near the primary recirculation region are displaced far from the step wall in the streamwise direction with Reynolds number increment due to the length increment of the primary recirculation region. This is because the skin friction coefficient is inversely proportional to the velocity.

2.6.3 Nusselt Number

The Nusselt number of SiO_2 nanofluid for different Reynolds numbers in range of $100 \leq Re \leq 500$ with q_w = 500 W/m^2, and $\emptyset$ = 4%, and d_p = 25 nm along the downstream wall is shown in Fig. 4b. It is shown the maximum peak in Nusselt number increases and transfers downstream of the step when Reynolds number increases. It can be seen also that the Reynolds number increases the convective current and it becomes stronger and the maximum value of the isotherms reduces. Moreover, the Nusselt number exponentially decreases from its optimum until it reaches a point approximately the exit where the vortex region is started. The results show that the flow with high Re number is found to have the lowest minimum peak of Nu number at the mixing region. Along this region, it is found that the SiO_2 nanofluid has higher Nusselt number at higher Reynolds number.

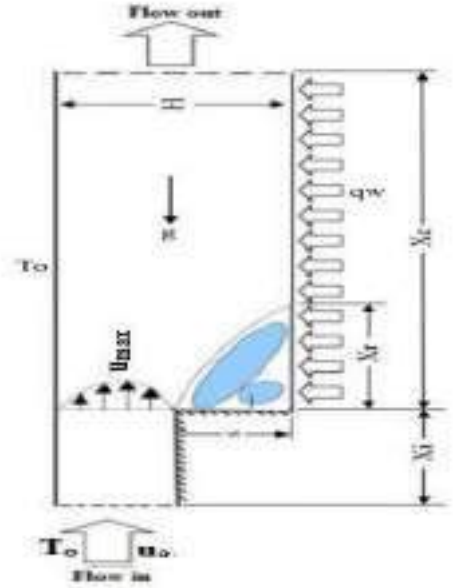

Fig. 1. Schematic Diagram for 2D BFS in a Vertical Channel

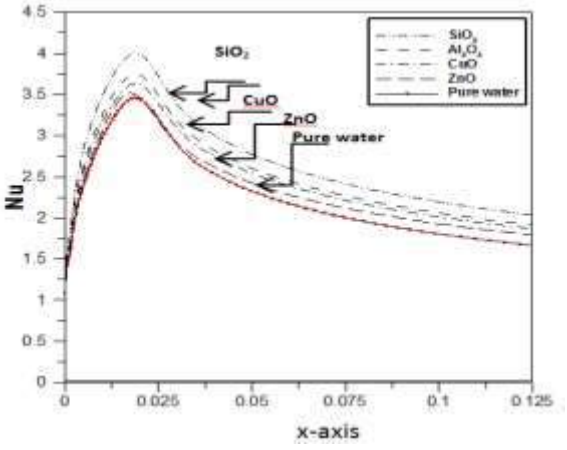

(a)

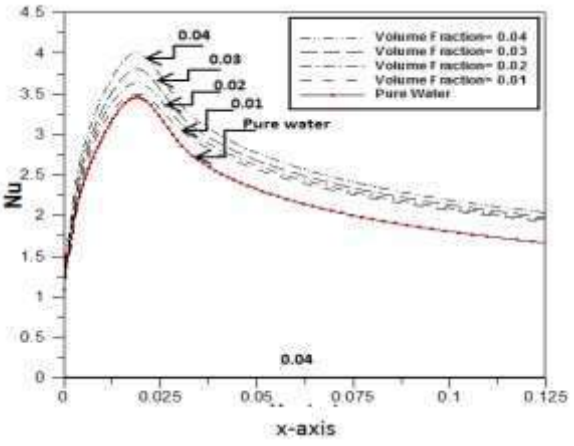

(b)

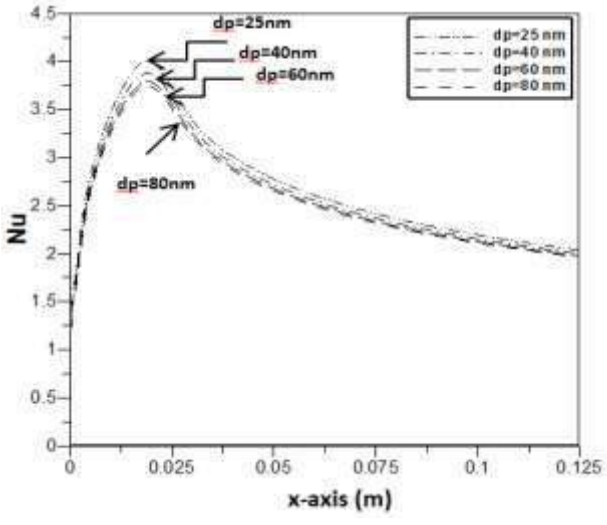

(c)

Fig. 2 The effect of nanofluids parameters along the downstream wall at Re = 100, qw = 500 W/m^2, Ø = 4%, and d_p = 25 nm for (a) different nanoparticle type, (b) different volume fractions, (c) different nanoparticle diameters

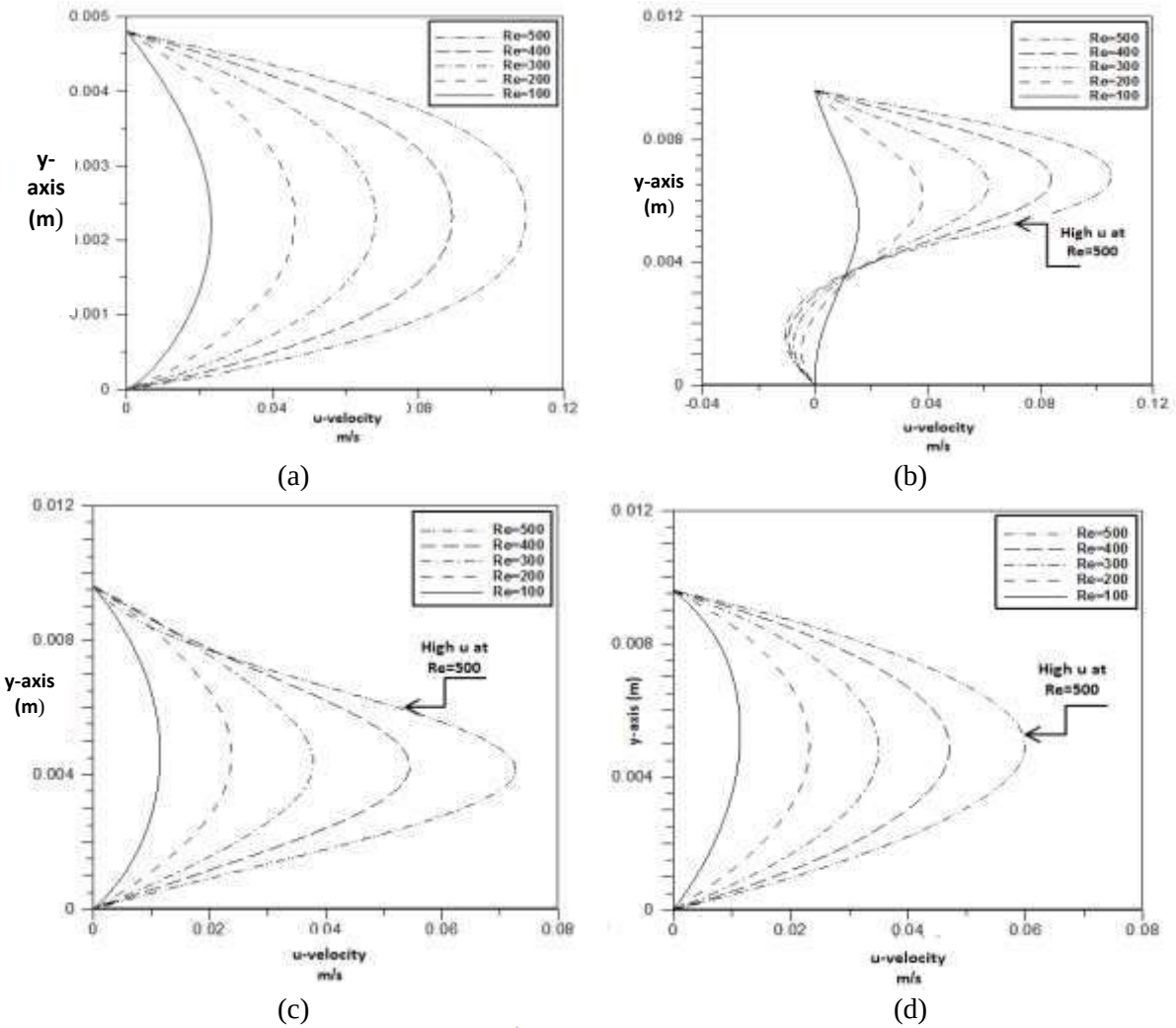

Fig. 3 Velocity Distributions of SiO_2 Nanofluid with $\emptyset$ = 4%, and d_p = 25 nm at Different Reynolds Numbers for q_w = 500 W/m^2 at (a) X/S = 0, (b) X/S = 1.8, (c) X/S = 12.82, (d) Exit

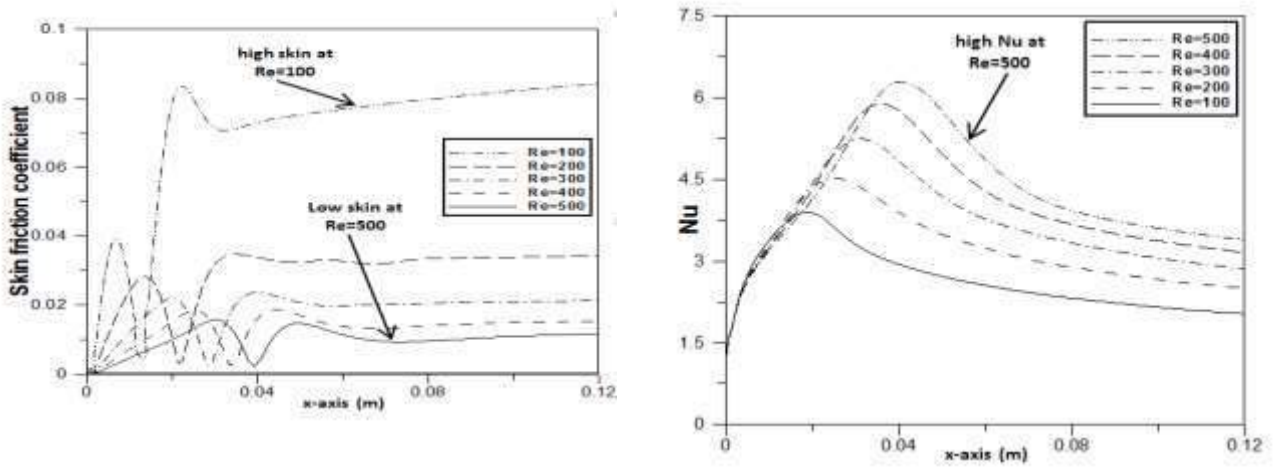

(a) (b)

Fig. 4 The effect of Re Number of SiO_2 Nanofluid with $\emptyset$ = 4%, and d_p = 25, q_w = 500 W/m^2 along the downstream wall (a) Skin friction coefficient, (b) Nusselt number

4- Conclusion

Numerical simulations for laminar mixed convection flow over two-dimensional vertical backward facing step were reported. The emphasis is given on the heat transfer enhancement resulting from various parameters, which include the type of nanofluids (Al_2O_3, CuO, ZnO, and SiO_2 with H_2O), nanoparticles diameter in the range of $25 \leq dp \leq 80$ nm, volume fraction (concentration) of nanoparticles in the range of $1\% \leq \emptyset \leq 4\%$. The Reynolds number of the backward facing step was in the range of $100 < Re < 500$. The downstream wall of the backward facing step was fixed at uniform heat flux boundary condition in the range of $100 \leq q_w \leq 600$ W/m^2 the channel has different step heights in the range of $3 \leq S \leq 5.8$ mm. The governing equations were solved utilizing finite volume method with certain assumptions and appropriate boundary conditions. In addition, the current study was examined the assisting and opposing flow conditions on the heat transfer characteristics.

Acknowledgements

The authors gratefully acknowledge the Al-Furat Al Awsat Technical University 'Iraq' for supporting this work.

References

[1] J. D'Adamo, R. Sosa, and G. Artana, "Active control of a backward facing step flow with plasma actuators," *Journal of Fluids Engineering*, vol. 136, p. 121105, 2014.
[2] A. Kumar and A. K. Dhiman, "Effect of a circular cylinder on separated forced convection at a backward-facing step," *International Journal of Thermal Sciences*, vol. 52, pp. 176-185, 2012.
[3] P. Williams and A. Baker, "Numerical simulations of laminar flow over a 3D backward-facing step," *International Journal for Numerical Methods in Fluids*, vol. 24, pp. 1159-1183, 1997.
[4] J. Nie and B. F. Armaly, "Three-dimensional convective flow adjacent to backward-facing step-effects of step height," *International journal of heat and mass transfer*, vol. 45, pp. 2431-2438, 2002.
[5] H. Mohammed, A. Al-Aswadi, N. Shuaib, and R. Saidur, "Convective heat transfer and fluid flow study over a step using nanofluids: a review," *Renewable and Sustainable Energy Reviews*, vol. 15, pp. 2921-2939, 2011.
[6] H. A. Hasan, K. Sopian, A. H. Jaaz, and A. N. Al-Shamani, "Experimental investigation of jet array nanofluids impingement in photovoltaic/thermal collector," *Solar Energy*, vol. 144, pp. 321-334, 2017.
[7] O. Alawi, C. N. Azwadi, S. Kazi, and M. K. Abdolbaqi, "Comparative study on heat transfer enhancement and nanofluids flow over backward and forward facing steps," *J. Adv. Res. Fluid Mech. Therm. Sci.*, vol. 23, pp. 25-49, 2016.
[8] E. Abu-Nada, "Application of nanofluids for heat transfer enhancement of separated flows encountered in a backward facing step," *International Journal of Heat and Fluid Flow*, vol. 29, pp. 242-249, 2008.

[9] D. John and J. Anderson, "Computational fluid dynamics: the basics with applications," *Mechanical Engineering Series. McGraw-HILL*, 1995.
[10] S. Patanker, "Numerical heat transfer and fluid flow. Hemisphere Publishing Corporation," *New York*, 1980.

LIST OF SYMBOLS

X_e	The wall downstream of the step
X_i	The wall upstream of the step
BFS	Backward double steps
S	The step it-self are considered as adiabatic surfaces
C_f	Skin friction coefficient = 2 τ_w / $\rho\, u_\infty^2$
C_p	Specific heat at constant pressure (J/kg K)
$C_{1\varepsilon}$, $C_{2\varepsilon}$, C_μ	Model constant = 144, 1.92, and 0.09, respectively
CFD	Computational Fluid Dynamic
d_f	Equivalent diameter of base fluid molecular (nm)
Dp	Nanoparticles diameter (nm)
FVM	Finite Volume Method
G_k	Turbulence kinetic energy production
H	Total duct height (m)
H	Convective heat transfer coefficient (W/m^2 K)
H_2O	Water
I	Turbulence intensity
K	Thermal conductivity of fluid (W/m K)
K	Turbulent kinetic energy
M	Molecular weight of base fluid
N	Avogadro number
Nu	Nusselt number (hH / k)
Pr	Prandtl number (ν/α)
P	Pressure
T	Temperature (K)
T_0	Constant temperature equivalent to the inlet fluid temperature
T_∞	Temperature at the inlet (K)
q_w	Heat flux (W/m^2)
u_∞	Velocity inlet (m/s)
u'	Velocity deviation from the mean in the x –direction (m/s)
v	Velocity component in the y – direction (m/s)
v'	Velocity deviation from the mean in the y - direction (m/s)
x	Streamwise coordinate direction
y	Transverse coordinate direction
Al_2O_3	Aluminum oxide
CuO	Copper oxide
SiO_2	Silicon dioxide
ZnO	Zinc oxide
Re	Reynolds number

Greek Symbols

α	Thermal diffusivity of fluid (m^2/s)
∞	Inlet conditions
K	Boltzmann constant, 1.381 $\times 10^{-3}$ J/K
B	Friction of liquid volume traveling with a particle
β	Thermal expansion coefficient (K^{-1})
μ	Dynamic viscosity of the fluid (N.m/s)
μ_t	Turbulent viscosity
V	Kinematic viscosity of the fluid (m^2/s)
ρ	Density of the fluid (kg/m^2)
ε	Dissipation rate of turbulent kinetic energy
σ_k , σ_ε	Turbulence model constant = 1, 1.3
$\emptyset$	Nanoparticles volume fraction
τ_w	Wall shear stress